VOLUME 32 · NUMBER 25 · SEPTEMBER 1 2014

JOURNAL OF CLINICAL ONCOLOGY

ORIGINAL REPORT

Emergence of New *ALK* Mutations at Relapse of Neuroblastoma

Gudrun Schleiermacher, Niloufar Javanmardi, Virginie Bernard, Quentin Leroy, Julie Cappo, Thomas Rio Frio, Gaelle Pierron, Eve Lapouble, Valérie Combaret, Frank Speleman, Bram de Wilde, Anna Djos, Ingrid Øra, Fredrik Hedborg, Catarina Träger, Britt-Marie Holmqvist, Jonas Abrahamsson, Michel Peuchmaur, Jean Michon, Isabelle Janoueix-Lerosey, Per Kogner, Olivier Delattre, and Tommy Martinsson

Author affiliations appear at the end of this article.

Published online ahead of print at www.jco.org on July 28, 2014.

In France, this study was supported by the Annenberg Foundation. Funding was also obtained from Site de Recherche Integré en Cancérologie/Institut National du Cancer (Grant No. INCa-DGOS-4654) and from the Comité d'évaluation et suivi des projets de Recherche de Transfert of Institut Curie. This study was also funded by the Associations Enfants et Santé, Association Hubert Gouin Enfance et Cancer, Les Bagouz à Manon, and Les Amis de Claire. Next-generation sequencing (NGS) experiments were conducted on the Institut Curie's ICGex NGS platform funded by the EQUIPEX Investissements d'Avenir program (Grant No. ANR-10-EQPX-03) and Grant No. ANR10-INBS-09-08 from the Agence Nationale de le Recherche and by the Canceropôle Ile-de-France. In Sweden, this work was supported by grants from the Swedish Cancer Society (Grant No. 12-817 TM), the Swedish Children's Cancer Foundation (Grant No. 10-129 TM), and the Swedish state through the LUA/ALF agreement. The Swedish part of the project was also supported by BioCARE, a National Strategic Research Program at the University of Gothenburg. In Belgium, this work was supported by the Fund for Scientific Research (Grants No. G.0198.08 and 31511809), the European Network for Cancer Research in Children and Adolescents: Seventh European Union Framework Programme (NoE No. 261474; Analyzing and Striking the Sensitivities of Embryonal Tumors: Seventh European Union Framework Programme, CP No. 259348), and the National Cancer Plan KPC_29_010 (Integrated biology-driven diagnostic and therapeutic management of neuroblastoma). This funding provided the necessary resources for the experimental phase of the study and for data analysis.

Both O.D. and T.M. contributed equally as senior authors of this study.

Authors' disclosures of potential conflicts of interest and author contributions are found at the end of this article.

Corresponding author: Gudrun Schleiermacher, MD, PhD, Department of Pediatric Oncology, Institut Curie, 26 rue d'Ulm, 75248 Paris Cedex 05, France; e-mail: gudrun.schleiermacher@curie.net.

0732-183X/14/3225w-2727w/$20.00

DOI: 10.1200/JCO.2013.54.0674

ABSTRACT

Purpose
In neuroblastoma, the *ALK* receptor tyrosine kinase is activated by point mutations. We investigated the potential role of *ALK* mutations in neuroblastoma clonal evolution.

Methods
We analyzed *ALK* mutations in 54 paired diagnosis–relapse neuroblastoma samples using Sanger sequencing. When an *ALK* mutation was observed in one paired sample, a minor mutated component in the other sample was searched for by more than 100,000× deep sequencing of the relevant hotspot, with a sensitivity of 0.17%.

Results
All nine *ALK*-mutated cases at diagnosis demonstrated the same mutation at relapse, in one case in only one of several relapse nodules. In five additional cases, the mutation seemed to be relapse specific, four of which were investigated by deep sequencing. In two cases, no mutation evidence was observed at diagnosis. In one case, the mutation was present at a subclonal level (0.798%) at diagnosis, whereas in another case, two different mutations resulting in identical amino acid changes were detected, one only at diagnosis and the other only at relapse. Further evidence of clonal evolution of *ALK*-mutated cells was provided by establishment of a fully *ALK*-mutated cell line from a primary sample with an *ALK*-mutated cell population at subclonal level (6.6%).

Conclusion
In neuroblastoma, subclonal *ALK* mutations can be present at diagnosis with subsequent clonal expansion at relapse. Given the potential of ALK-targeted therapy, the significant spatiotemporal variation of *ALK* mutations is of utmost importance, highlighting the potential of deep sequencing for detection of subclonal mutations with a sensitivity 100-fold that of Sanger sequencing and the importance of serial samplings for therapeutic decisions.

J Clin Oncol 32:2727-2734. © 2014 by American Society of Clinical Oncology

INTRODUCTION

Current treatment approaches in cancer often lead to initial response followed by secondary progression that presents a therapeutic challenge because of resistance to conventional chemotherapy treatment.[1] Thus, genetic characterization of cancer cells provides invaluable information for the identification of molecular therapeutic targets. Importantly, particular genetic alterations may be selected for or emerge during treatment.[2,3] Subclonal driver mutations might play a role in tumor progression, and the presence of driver mutation–harboring subclones at diagnosis, which might expand at relapse, has been linked to adverse outcomes.[2-5]

In neuroblastoma, the most frequent extracranial solid cancer of early childhood, tumor progression is often associated with limited therapeutic possibilities, underlining the need of molecular analyses.[6] Genetic alterations in neuroblastoma at diagnosis mainly concern copy number alterations, with *MYCN* amplification in 20% to 25% of cases, and other copy number changes over extensive chromosome regions.[6-11] Only a few recurrently altered genes, such as chromatin-remodeling or neuritogenesis genes, have been reported, targeted by either small interstitial structural alterations or mutations.[8-10] Activating point mutations in the tyrosine kinase domain of *ALK*, the most frequent mutations in neuroblastoma, are detected at diagnosis in approximately 8% to 10% of patients and play an important role in neuroblastoma oncogenesis.[12-17]

These alterations can be targeted using ALK inhibitors, and in vitro and in vivo models have

indicated their potential usefulness in the presence of an activating *ALK* mutation.[18-20] A phase I/II study of crizotinib, a dual ALK/MET inhibitor, suggests possible efficacy in neuroblastoma harboring *ALK* mutations.[21] Thus, it will be crucial to define treatment indications depending on the precise molecular characterization of *ALK* mutations in neuroblastoma.

Recently a relapse-specific *ALK* mutation has been described, correlating with unresponsiveness to therapy and indicating that the determination of the *ALK* status at tumor progression is critical.[22] However, the actual frequency of *ALK* mutations at relapse has not yet been studied. We have studied 54 paired diagnosis–relapse neuroblastoma samples to analyze the frequency of *ALK* mutations at relapse and to define their potential role in clonal evolution.

METHODS

Patients

Patients with neuroblastoma of all stages were included in this study if tumor samples collected in the participating laboratories both at diagnosis and at relapse were available (24 Swedish, 28 French, and two Belgian patients; Data Supplement). Patients were treated according to relevant national or international treatment protocols (Data Supplement). Ethics approval of protocols was obtained according to national guidelines, and written informed consent was obtained from parents according to national law. In France, this study was authorized by the ethics committee (Comité de Protection des Personnes Sud-Est IV), L07-95, and L12-171. In Belgium, the ethics committee EC/2006-124 approved this work. In Sweden, this study was authorized by the local ethical committees 09-1368, 09-473 (Gothenburg), and 07-069 (Uppsala). Diagnosis samples were obtained from the primary tumor site in the majority of patients (92%) according to clinical guidelines. Relapse samples were obtained from progressing/relapsed primary tumor in 68% of patients and from metastatic sites in 32% of patients (Data Supplement).

Sanger Sequencing of the ALK Receptor Tyrosine Kinase Domain

Paired diagnosis–relapse tumor samples were included if the samples contained more than 50% tumor cells by pathologic examination. After DNA extraction using standard procedures, mutations of the *ALK* receptor tyrosine kinase domain were searched for by Sanger sequencing (Data Supplement).[12,15] *ALK* mutation in one relapse sample has been previously described.[22] Cell lines CLB-Ba and CLB-Ma and the corresponding primary sample (massively invaded bone marrow and primary tumor, respectively) were also studied.[15] Cell lines CLB-Car, SKNDZ, SKNAS, and SJNB12 served as controls.[15]

Sequencing of ALK Exonic Regions with IonTorrent Personal Genome Machine Technology

Sequencing libraries were built with the IonFragment Library Kit for AB Library Builder System following the manufacturer's recommendations (Life Technologies, Grand Island, NY). Briefly, 10 to 100 ng of polymerase chain reaction products of relevant *ALK* exonic regions (exon 23: chr2:29443486 to 29443776; exon 25: chr2:29432565 to 29432822) were end-repaired, and IonTorrent bar-coded adapters were ligated at the 5′ and 3′ extremities. After a brief polymerase chain reaction amplification and quality control, equal quantities of each library were pooled and sequencing templates were prepared on an IonOneTouch system with the IonOneTouch 200 Template Kit DLv2 (Life Technologies). The number of libraries sequenced per 318 Ion chip was determined to achieve a depth of over 100,000× for the amplicons in every sample (Data Supplement).

Bioinformatics Detection of Variations

Reads were aligned via the TorrentSuite Software v3.4.1 (Life Technologies) with default parameters. Variant calling was not used because variations at low frequencies were to be identified and standard procedures would have filtered them. A custom approach was required to highlight the variations with low frequencies, some occurring with a frequency of less than 1%. Using DepthOfCoverage functions of the Genome Analysis Toolkit v2.13.2 (Broad Institute, Cambridge, MA), we focused on coverage analysis of A, C, G, and T at chr2:29432646 to 29432674 (29 bp) and chr2:29443686 to 29443705 (20 bp) (Human Genome Browser, http://genome.ucsc.edu/; hg19) to analyze the 10 bases directly surrounding the *ALK* hotspots Y1278 and R1275 (exon 25) and F1174 (exon 23), respectively. Only reads with mapping quality of 8 or higher and bases having a base quality of 17 or more were taken into account according to Personal Genome Machine (PGM; Life Technologies) criteria for quality filtering to avoid low-quality data. To determine the background level of variability at the studied regions, control samples were included in the analysis. In the controls for each position, the frequency for each base was calculated. For a sample to be studied at a given position, the frequencies of the bases at the given position were then compared with those observed in the controls. Statistical analyses were performed with the R statistical software (http://www.R-project.org). Fisher's exact two-sided tests were performed to compare percentages of bases between the data sets (ie, between a case and the controls). To limit false-positive prediction of differences between cases and controls, Bonferroni's correction was applied. Statistically significant increases in the percentages of bases were considered for $P < .05$.

RESULTS

To determine the frequency of *ALK* mutations at relapse, we performed Sanger sequencing of the *ALK* receptor tyrosine kinase domain in a series of 54 paired diagnosis–relapse neuroblastoma samples. *ALK* mutations were observed in nine of 54 diagnostic samples (Tables 1 and 2). For all nine cases, the same mutation was also detected by Sanger sequencing in a sample at relapse. In one case (NB1224), an *ALK* mutation, detected at diagnosis, was seen at relapse in only one of several samples. Indeed, the *ALK* mutation was found in only one of the stroma-poor tumor nodules and not in the stroma-rich tissue surrounding the nodules (Fig 1). A germline *ALK* mutation was observed in only one case (NB0073).

At relapse, new *ALK* mutations were also detected by Sanger sequencing in five additional cases (Table 1). These were a F1174L mutation (exon 23) in two cases, a F1174S mutation (exon 23) described previously in one case,[22] and a Y1278S mutation and R1275Q mutation (exon 25) in the other two cases.

In cases where *ALK* mutations were detected by Sanger sequencing in only one of all available tumor samples, we determined whether the *ALK* mutation might have gone undetected in the other samples as a result of a limit in sensitivity of the Sanger technique. We used the IonTorrent PGM technique to resequence the relevant hotspots in all available tumor samples of case NB1224 and of four of five cases with an *ALK* mutation seen only at relapse (NBG12, NBG17, NB0308, and NB1382). For the fifth case, no sufficient material was available for the PGM analysis. Using the 318 chip (Life Technologies), a high coverage was achieved for all cases at the resequenced regions, with more than 100,000 reads per position after application of bioinformatics filters (Data Supplement).

To determine the sensitivity of our technique, in a first step, the background variability resulting from the PGM sequencing was calculated for the control cell lines in the studied region. The mean overall coverage for the control cell lines was more than 175,000×. The mean overall background variability was 0.034% ± 0.035% for each base, except the reference base, with no significant outlier (Data Supplement). To determine the expected sensitivity, we then calculated which number of reads would be considered statistically different

Table 1. Clinical and Tumor Genetic Data of Patients With *ALK* Mutations

Patient No.	Clinical Information					*ALK* Mutation			*ALK* Detection by Sanger Sequencing			*ALK* Detection by PGM (% of total reads)	
	Age at Diagnosis (months)	Stage (INSS)	Interval From Diagnosis to Relapse (months)	Relapse Type	Follow-Up (months from diagnosis)	Outcome	Genomic Profile (at diagnosis)	AA Change	Position and Mutation	Germline	Diagnosis	Relapse	Diagnosis	Relapse
NBG03	50	4	23	loc	29	DOD	MNA	F1174L	29443695 (TTC>TTA)	Neg	Pos	Pos	ND	ND
NBG14	90	4	10	loc	55	NED	S	F1174L	29443695 (TTC>TTA)	Neg	Pos	Pos	ND	ND
NBG21	41	2b	11	met	17	DOD	MNA	F1174L	29443695 (TTC>TTA)	Neg	Pos	Pos	ND	ND
NB0175	101	2b	93	loc + meta	150	DOD	S	Y1278S	29432655 (TAC>TCC)	Neg	Pos	Pos	ND	ND
NB0399	0.2	4s	6	meta	136	DOD	N	R1275Q	29432664 (CGA>CAA)	Neg	Pos	Pos	ND	ND
NB0824	3	4	3	meta	16	DOD	N	F1174L	29443695 (TTC>TTA)	Neg	Pos	Pos	ND	ND
NB1269	14	4	10	loc	11	DOD	S	L1196M	29443631 (CTG>ATG)	Neg	Pos	Pos	ND	ND
NB1224	24	2b	4	loc	14	NED	S	R1275Q	29432664 (CGA>CAA)	Neg	Pos	Pos	14.164*	28.536*
NB0073	3	4s	7	meta	272	NED	N	T1151R	29445273 (ACG>AGG)	Pos	Pos	Pos	ND	ND
NBG05	37	4	45	loc + meta	50	DOD	MNA	R1275Q	29432664 (CGA>CAA)	Neg	Neg	Pos	ND	ND
NBG12	12	4	9	meta	9	DOD	S	F1174S	29443696 (TTC>TCC)	Neg	Neg	Pos	0.034	90.734*
NBG17	29	4	13	meta	24	DOD	MNA	F1174L	29443695 (TTC>TTA)	Neg	Neg	Pos	0.798*	26.113*
NB1382	4	4	51	loc + meta	63	DOD	S	Y1278S	29432655 (TAC>TCC)	Neg	Neg	Pos	0.011	33.613*
NB0308	3	2b	21	loc	93	NED	N	F1174L	29443695 (TTC>TTA/TTG)	Neg	Neg	Pos	8.150* (C > A)	19.125* (C > G)

NOTE. For all patients with *ALK* mutations detected at diagnosis by Sanger sequencing, mutations were also detected by Sanger at relapse. In five cases, mutations were detected by Sanger at relapse only, two of which (NB0308 and NBG17) could be shown to harbor *ALK* mutations in a smaller fraction of cells or subclones at diagnosis as evidenced by PGM deep sequencing. Furthermore, for a cell line harboring an *ALK* mutation, the mutation was observed in a subclone of cells in the primary sample (CLB_Ba).

Abbreviations: DOD, dead of disease; INSS, International Neuroblastoma Staging System; loc, local relapse; meta, metastatic relapse; MNA, *MYCN* amplification; N, numerical chromosome alterations; ND, not done; NED, no evidence of disease; Neg, negative; PGM, Personal Genome Machine; Pos, positive; S, segmental chromosome alterations.

*Signifies a base frequency as detected by PGM with a statistically significant difference from the controls.

Table 2. Patient Data According to Cell Line

Cell Line	Age at Diagnosis (months)	Stage (INSS)	Primary Sample (% tumor cells)	Tissue From Which Cell Line Was Established	Follow-Up From Diagnosis (months)	Outcome	Genomic Profile	AA Change	Position and Mutation	*ALK* Detection by Sanger Sequencing		*ALK* Detection by PGM (% of total reads)	
										Primary Sample	Cell Line	Primary Sample	Cell Line
CLB_Ma	9	4	Abdominal tumor (50%)	Bone marrow	16	DOD	MNA	F1174L	29443695 (TTC>TTA)	Neg	Pos	0.027	44.432*
CLB_Ba	27	4	Bone marrow (80%)	Bone marrow	117	NED	MNA	F1174L	29443697 (TTC>CTC)	Neg	Pos	6.609*	32.378*

Abbreviations: DOD, dead of disease; INSS, International Neuroblastoma Staging System; MNA, *MYCN* amplification; NED, no evidence of disease; Neg, negative; PGM, Personal Genome Machine; Pos, positive.
*Signifies a base frequency as detected by PGM with a statistically significant difference from the controls.

from the background. Bonferroni's correction was applied, because multiple tests were performed for each base at each position. Considering a mean coverage of 175,000×, a variation supported by 296 reads, or observed with a frequency of 0.17%, would result in a statistically significant difference from the controls (two-sided Fisher's exact test). For the studied tumor samples, the background variability was not different from that of the controls, except the mutation hotspots, and no mutations outside the mutation hotspots were detected.

In a next step, to analyze more precisely the mutation hotspots, the percentage of bases at coordinates 29443696, 29443695, 29432664, and 29432655, corresponding to the mutations F1174S(T>C) in NBG12, F1174L(C>A) in NBG17 and NB0308, R1275Q(G>A) in NB1224, and Y1278S(A>C) in NB1382, respectively, were studied in detail in the respective samples (Table 3). For each case, the frequency of bases at a given position was compared with frequencies observed in the controls (two-sided Fisher's exact test; Tables 1, 2, and 3). As expected, the PGM analysis detected all mutations seen by Sanger sequencing and enabled further precision regarding their allele frequency. In case NBG12, PGM analyses of the previously described homozygous F1174S(T>C) mutation indicated the presence of the mutated allele in 90.7% and of the wild-type allele in 9.2% of the reads in the relapse sample (Table 1).[22] Indeed, for this case, as previously reported, single nucleotide polymorphism arrays clearly documented copy neutral loss of heterozygosity of chromosome 2p, indicating a duplication of the mutated allele, with the wild-type allele corresponding to contaminating normal tissue.[22]

PGM analysis further established the *ALK* status in cases for which Sanger sequencing revealed an *ALK* mutation in only one of the paired samples. In two cases with an *ALK* mutation detected in the relapse sample (NBG12 and NB1382), analysis of the diagnosis sample by PGM showed no statistically significant difference between the frequency of the base corresponding to the mutated allele and the background (Table 3). Interestingly, in two other cases (NBG17 and NB0308), a base corresponding to a mutated allele, although not detected by Sanger, was observed in the diagnosis sample in a significantly higher frequency than the controls (Fisher's exact, $P < 10^{-16}$; Tables 1 and 3; Fig 2). In case NBG17, the mutated allele was detected in the diagnosis sample at 0.798%, indicating the presence of an *ALK*-mutated subclone at diagnosis (Fisher's exact test, $P < 10^{-16}$). Strikingly, in case NB0308, two distinct *ALK* mutations were detected at diagnosis and at relapse; at diagnosis, a mutation was observed in 8.15%, below the detection limit of Sanger sequencing. This mutation was not seen at relapse. At relapse, a different mutation was observed in 19.125% (Fisher's exact test, $P < 10^{-16}$; Data Supplement). These mutations led to the same AA change, indicating a mutation switch between diagnosis and relapse with an expected identical functional consequence.

Finally, to search for further evidence of clonal selection of *ALK*-mutant cells, two established cell lines (CLB-Ma and CLB-Ba), with a previously described F1174L mutation observed by Sanger sequencing, were compared with the corresponding primary sample.[15] In case CLB-Ma, PGM analysis of the primary tumor tissue Ma(PT) did not reveal a higher frequency of the mutation base compared with the controls, indicating that in the studied sample, no *ALK*-mutated subclone could be detected (Tables 2 and 3). However, the cell line was established from invaded bone marrow. Because no sample of this bone marrow was available for PGM analysis, it cannot be excluded that an *ALK*-mutated subclone might have been present in the metastatic site. For CLB-Ba, PGM analysis of the primary sample [invaded bone marrow, Ba(PT_BM)] from which the cell line was directly established revealed the presence of the mutation in 6.6% of the studied DNA fragments, indicating the presence of an *ALK*-mutated subclone in the primary sample, which then expanded during establishment of the cell line harboring the known *ALK* mutation in all cells (Tables 2 and 3; Fig 2).

DISCUSSION

With the increasing importance of targeted therapies, full characterization of molecular genetic events in cancer cells becomes crucial. The new, high-resolution next-generation sequencing techniques now enable the evaluation of biomarkers for more precise studies of clonal evolution in sequential samples from the same patient.

In neuroblastoma, only few studies have analyzed the genetic alterations at relapse, with no alterations specific for relapse described to date.[11] One recent report has described a relapse-specific *ALK* mutation.[22] We now report on the search for *ALK* mutations in 54 paired diagnosis–relapse neuroblastoma samples. In this study of samples from patients who experienced relapse, we observed *ALK* mutations at diagnosis in 17% of the patients, suggesting that at diagnosis, in patients who experience relapse, the incidence of *ALK* mutations might be higher than that reported in the overall population.[13] Furthermore, we demonstrate an emergence of *ALK* mutations

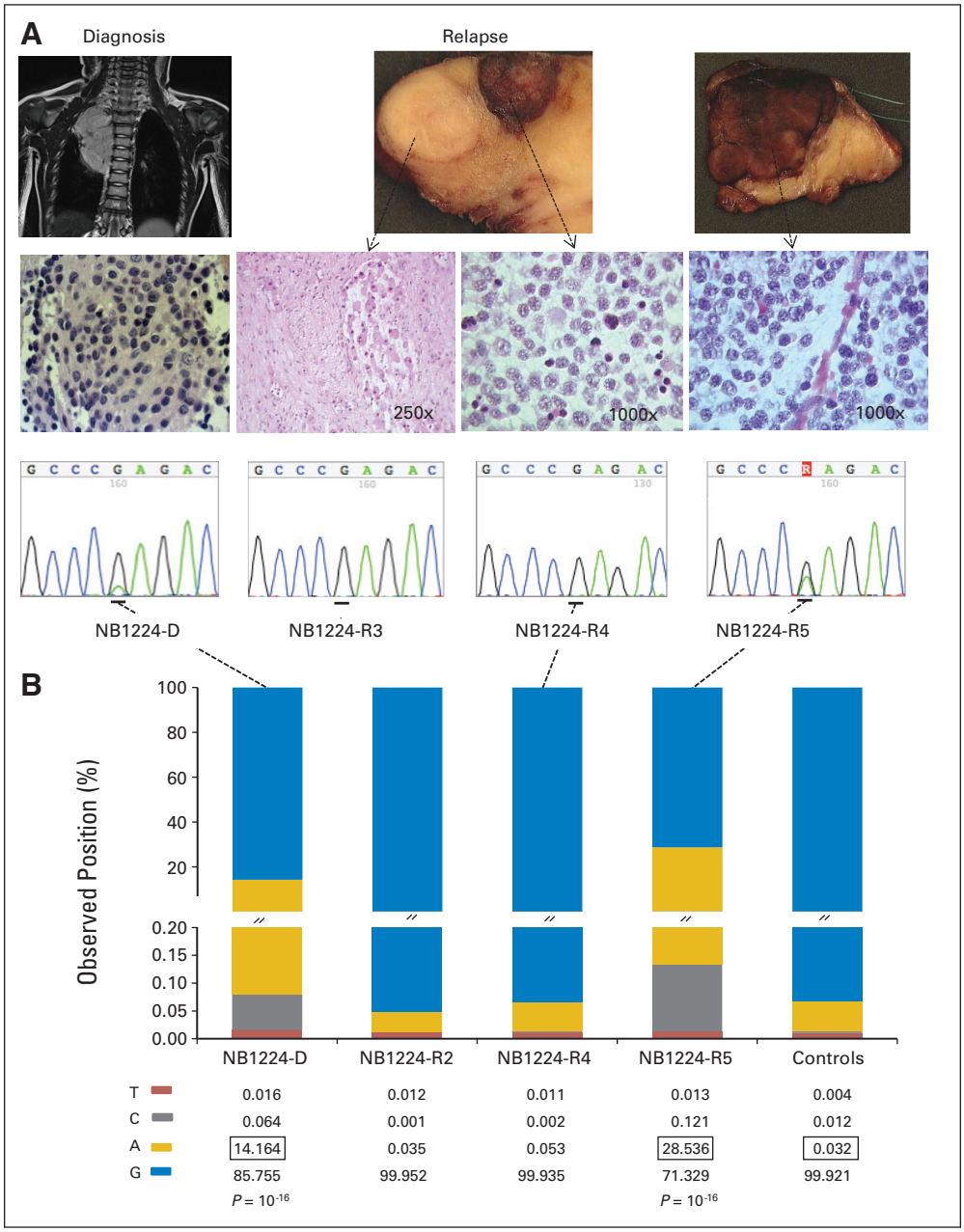

Fig 1. *ALK* status in different samples of NB1224. (A) Macroscopic and microscopic aspect of the tumor at different time points and results of Sanger sequencing searching for *ALK* mutation. The position corresponding to the mutation R1275Q is underlined (chr2:29432664). At diagnosis, a localized International Neuroblastoma Risk Group Staging System L2 neuroblastoma, stroma poor, poorly differentiated, with high mitosis-karyorrhexis index (MKI), was observed. Sanger sequencing showed the presence of an R1275Q (CGA>CAA) mutation (diagnostic sample, NB1224-D). The patient received two courses of chemotherapy and was then observed. The patient experienced local progression 4 months after first-line chemotherapy. At relapse, a biopsy of the tumor was first performed (relapse sample, NB1224-R2). After additional courses of chemotherapy, surgical resection revealed a postchemotherapeutic tumor, classified as a peripheral neuroblastic tumor, not otherwise specified, according to INPC recommendations. The postchemotherapy effects were minimal, without any necrosis being observed, and this tumor was indeed histologically composed of a stroma-rich component (relapse sample, NB1224-R3) and of several stroma-poor nodules with numerous neuroblasts, poorly differentiated; in one nodule, the MKI was low (relapse sample, NB1224-R4); in another nodule, the MKI was high (relapse sample, NB1224-R5). At progression, the R1275Q (CGA>CAA) mutation was found only in the nodule corresponding to neuroblastoma, stroma poor, poorly differentiated, MKI high (NB1224-R5), and not in the other nodule or in the stroma-rich component. (B) Results of Personal Genome Machine (PGM) sequencing of case NB1224 at position chr2:29432664. Diagnostic sample: NB1224-D; relapse samples: NB1224-R2, NB1224-R4, and NB1224-R5. The observed frequencies of bases at the studied position are indicated in the graph. For the controls, the mean of the base percentages for the four control cell lines is indicated. Statistically significant differences between the sample and controls of base frequencies for the base A, corresponding to the mutation, are circled, and the results of the Fisher's exact tests are indicated. PGM sequencing confirmed the results observed with Sanger sequencing, with presence of an R1275Q (CGA>CAA) mutation in samples NB1224-D and NB1224-R5. The base corresponding to the mutated allele did not exceed the background variability in the other tumor fragments analyzed (NB1224-R2 and NB1224-R4).

at the time of relapse. This finding is of utmost clinical importance given the possibility of targeted treatment with ALK inhibitors and the fact that *ALK* mutations are considered an important predictive molecular marker.[21]

Sanger sequencing is reported to detect 20% to 30% of mutated alleles in a wild-type background.[23,24] For sensitivity estimation, contamination with normal cells should be considered. For this study, contamination of tumor samples by normal cells of up to 50% was

Table 3. Base Frequencies at the Coordinates of Interest in Samples Analyzed by Deep-Sequencing PGM

Chromosome Position and Patient No.	No. of Reads	A		C		G		T	
		%	*P*	%	*P*	%	*P*	%	*P*
Chr2:29432655 (A)									
NB1382-D	226,371	99.954	1.00	0.011	1.00	0.031	1.00	0.004	1.00
NB1382-R	179,938	66.326	$< 10^{-16}$	33.613*	$< 10^{-16}$	0.032	1.00	0.029	$< 10^{-14}$
Controls (n = 4)			SD		SD		SD		SD
Total of all reads	701,987	99.941	NA	0.012	NA	0.043	NA	0.004	NA
Mean		99.942	.00249	0.012	.00467	0.043	.00307	0.004	.00251
Chr2:29432664 (A)									
NB1224-D	258,308	14.164*	$< 10^{-16}$	0.064	< .001	85.755	$< 10^{-16}$	0.016	1.00
NB1224-R2	302,176	0.035	1.00	0.001	1.00	99.952	1.00	0.012	1.00
NB1224-R4	318,313	0.053	1.00	0.002	1.00	99.935	1.00	0.011	1.00
NB1224-R5	302,918	28.536*	$< 10^{-16}$	0.121	< .001	71.329	$< 10^{-16}$	0.013	1.00
Controls (n = 4)			SD		SD		SD		SD
Total of all reads	703,934	0.038	NA	0.001	NA	99.952	NA	0.009	NA
Mean		0.032	.00249	0.012	.00467	99.921	.00307	0.004	.00251
Chr2:29443695 (C)									
NB0308-D	183,381	8.150*	$< 10^{-16}$	91.799	$< 10^{-16}$	0.003	1.00	0.048	1.00
NB0308-R	241,456	0.019	.0830	80.754	$< 10^{-16}$	19.125*	$< 10^{-16}$	0.101	$< 10^{-9}$
NBG17-D	104,176	0.798*	$< 10^{-16}$	99.175	1.00	0.003	1.00	0.025	1.00
NBG17-R1	125,167	26.113*	$< 10^{-16}$	73.796	$< 10^{-16}$	0.008	1.00	0.083	$< 10^{-5}$
NBG17-R2	131,857	30.921*	$< 10^{-16}$	68.963	$< 10^{-16}$	0.005	1.00	0.111	$< 10^{-15}$
Ma(PT)	127,449	0.027	1.00	99.899	1.00	0.002	1.00	0.072	.0147
CLB_Ma	135,813	44.432*	< .001	55.157	$< 10^{-16}$	0.018	< .001	0.393*	$< 10^{-16}$
Controls (n = 4)			SD		SD		SD		SD
Total of all reads	496,439	0.046	NA	99.914	NA	0.001	NA	0.039	NA
Mean		0.049	.0201	99.912	.0214	0.001	< .001	0.039	.00252
Chr2:29443696 (T)									
NBG12-D	133,215	0.002	1.00	0.034	1.00	0.002	1.00	99.963	1.00
NBG12-R	124,488	0.007	1.00	90.734*	$< 10^{-16}$	0.085	$< 10^{-16}$	9.175	$< 10^{-16}$
Controls (n = 7)			SD		SD		SD		SD
Total of all reads	527,325	0.003	NA	0.044	NA	0.007	NA	99.946	NA
Mean		0.002	.00243	0.044	.00664	0.007	.00351	99.947	.00780
Chr2:29443697 (T)									
Ba(PT_BM)	198,359	0.046*	$< 10^{-16}$	6.609*	$< 10^{-16}$	0.003	.990	93.342	< .001
CLB_Ba	176,260	0.400*	$< 10^{-16}$	32.378*	$< 10^{-16}$	0.003	.989	67.22	< .001
Controls (n = 4)			SD		SD		SD		SD
Total of all reads	516,559	0.005	NA	0.015	NA	0.011	NA	99.969	NA
Mean		0.006	.00146	0.015	.00191	0.010	.0181	99.970	.0208

NOTE. The base corresponding to the reference genome (Human Genome Browser, http://genome.ucsc.edu/; hg19) is indicated at a given coordinate. For a sample to be analyzed, the total number of high-quality reads obtained by PGM deep sequencing is indicated, and the percentage of reads supporting each base (A, C, G, T) is shown. Values reported for controls are calculated from the total number of reads for all controls at the given position. The mean base frequencies calculated from the controls, with their standard deviation, are also indicated. For each case, the *P* value refers to the comparison (two-sided Fisher's exact test) of the base frequency observed in the studied sample to that observed in the controls.

Abbreviations: D, diagnosis; NA, not available; PGM, Personal Genome Machine; R, relapse; SD, standard deviation.

*Variations with a statistically significant difference from controls.

tolerated, and thus, it is expected that in these samples heterozygous mutations occurring in all tumor cells, present in 25% of all analyzed DNA fragments, would be at the limit of detection by Sanger sequencing. To search for *ALK* mutations with a higher sensitivity than that of Sanger, deep sequencing with an extremely high coverage over the region of interest ($> 100{,}000\times$) was performed. Limitations in the detection of low-frequency variations are linked to the IonTorrent PGM sequencing technique, which has an underlying error rate depending on the base, its position, and the surrounding bases. Indeed for IonTorrent PGM sequencing of the human genome, the overall error rate in lower coverage experiments, including mismatches, deletions, and insertions, has been reported to be approximately 0.019%, which might vary strongly according to the genome structure and the presence or absence of homopolymers and might be linked to sequencing errors as a result of polymerase slippage, errors in the chemistry, or other errors.[25,26] Future technologic improvements may reduce this background variability. In this high-coverage analysis, the background variability was 0.034% per base, resulting in a sensitivity of 0.17%, 100-fold that of Sanger sequencing.

This deep-sequencing approach indicated that *ALK* mutations might occur as subclones at neuroblastoma diagnosis with secondary expansion, contributing to a selective advantage during tumor progression. Our data also suggest that, in some instances, *ALK*-mutated and -nonmutated cells might coexist in an equilibrium. The expansion of an *ALK*-mutated clone on treatment may suggest a preferential cytotoxic effect on *ALK*-nonmutated clones.

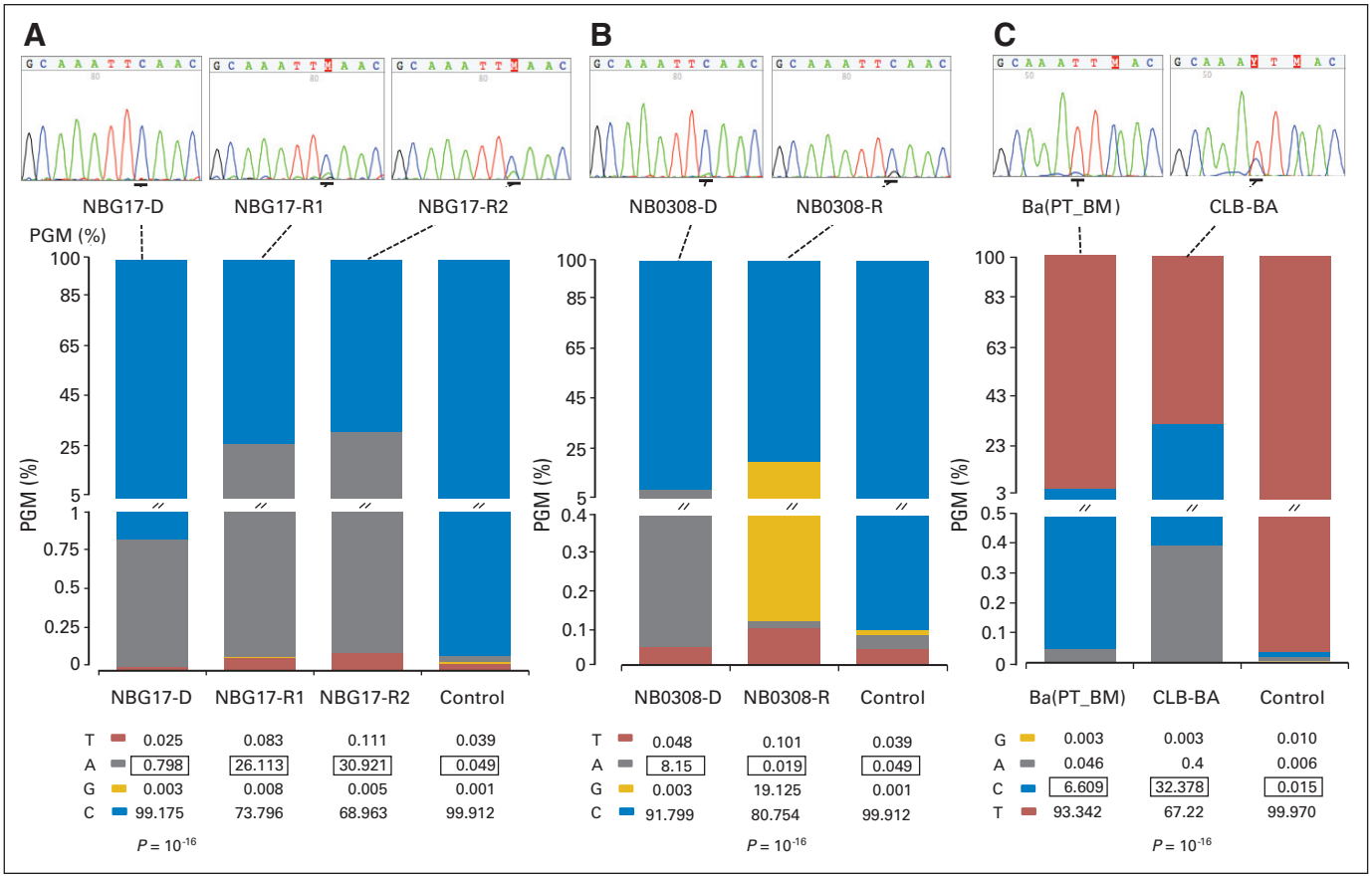

Fig 2. *ALK* mutations detected at the time of diagnosis and relapse using Sanger sequencing (upper panels) and Personal Genome Machine (PGM) deep sequencing (lower panels). For each case, -D and -R refer to samples obtained at diagnosis and at relapse, respectively. Base frequencies at the studied position for the sample and the controls, determined by IonTorrent PGM, are indicated; statistically significant differences of base frequencies between the sample and controls are circled, and the result of the Fisher's exact is indicated (lower panels). (A) Patient NBG17: Sanger sequencing showed the presence of an *ALK* mutation F1174L (TTC>TTA) in two sequential samples obtained at relapse that was not detected at diagnosis. PGM (position Chr2:29443695) detected the *ALK* mutation in 0.798% at diagnosis, indicating the presence of an *ALK*-mutated subclone at diagnosis. (B) Patient NB0308: Sanger sequencing showed a clear F1174L mutation at relapse. Deep sequencing confirms the F1174 (TTC>TTG) mutation at relapse (position Chr2:29443695), with a frequency of 19.125%. Furthermore, a different F1174L mutation (TTC>TTA) is detected in the diagnostic sample, at 8.15%, leading to the same amino acid change and indicating a mutation switch between diagnosis and relapse. (C) CLB-Ba: Sanger sequencing detected a F1174L mutation (TTC>CTC; chr2:29443697) in the established cell line but not in the primary tumor sample Ba(PT_BM) (bone marrow from which the cell line was derived, reported to harbor approximately 80% of tumor cells). PGM reveals the presence of the *ALK* mutation in 6.609%, which is statistically significantly different from the background variability and indicating the presence of the mutation in a subclone of the infiltrated bone marrow.

This study also reveals the important observation, in one case, of two different *ALK* mutations at diagnosis and relapse, both leading to the same AA change. Possible explanations include the presence of the second mutation in a minor subclone at diagnosis below the detection limit of our technique; spatial heterogeneity throughout the tumor, with one mutation occurring in one tumor section and another in a different tumor section; or a new occurrence of a mutation not present at diagnosis. The same AA change having potentially occurred independently twice in tumor development suggests that these mutations emerged as a result of a possible addiction to the functional modifications linked to the *ALK* mutation.

The detailed knowledge of the *ALK* status in neuroblastoma is important in view of the availability of targeted therapy, with new-generation, more selective, higher affinity ALK-specific agents currently being developed.[18] The identification of an *ALK* mutation in a tumor sample can be considered as a positive predictive marker for efficacy of ALK-targeted treatment.[18,19,21] Additional studies are now necessary to determine how the presence of *ALK* mutations in tumor subclones might influence ALK-targeted treatment efficacy.

Our study leads to two crucial conclusions. First, the observation of five of 54 new *ALK* mutations at relapse suggests that the frequency of *ALK* mutations may be higher at relapse than at diagnosis, requiring further validation in larger cohorts. Second, subclones harboring *ALK* mutations may contribute to tumor evolution and relapse. This has major clinical implications. Our findings provide proof of principle that the systematic application of new, more sensitive deep-sequencing techniques in neuroblastoma is of clinical interest and should be considered on diagnostic samples. Furthermore, *ALK* mutations should be searched for not only at diagnosis but also at relapse when considering ALK-targeted therapies. Thus, although clinicians historically have been reluctant to prescribe invasive procedures for relapse in high-risk neuroblastoma, our findings implicate a change in medical practice in favor of tumor sampling even at relapse, and repeated tumor sampling should become a new standard of care.

AUTHORS' DISCLOSURES OF POTENTIAL CONFLICTS OF INTEREST

The author(s) indicated no potential conflicts of interest.

AUTHOR CONTRIBUTIONS

Conception and design: Gudrun Schleiermacher, Niloufar Javanmardi, Julie Cappo, Thomas Rio Frio, Per Kogner, Olivier Delattre, Tommy Martinsson
Financial support: Gudrun Schleiermacher, Jean Michon, Per Kogner, Olivier Delattre, Tommy Martinsson
Administrative support: Gudrun Schleiermacher, Jean Michon, Per Kogner, Tommy Martinsson
Provision of study materials or patients: Gudrun Schleiermacher, Gaelle Pierron, Eve Lapouble, Valérie Combaret, Bram de Wilde, Fredrik Hedborg, Catarina Träger, Per Kogner, Olivier Delattre, Tommy Martinsson
Collection and assembly of data: Gudrun Schleiermacher, Niloufar Javanmardi, Virginie Bernard, Quentin Leroy, Julie Cappo, Thomas Rio Frio, Gaelle Pierron, Eve Lapouble, Valérie Combaret, Frank Speleman, Bram de Wilde, Anna Djos, Ingrid Øra, Fredrik Hedborg, Catarina Träger, Britt-Marie Holmqvist, Jonas Abrahamsson, Michel Peuchmaur, Jean Michon, Isabelle Janoueix-Lerosey, Per Kogner, Olivier Delattre, Tommy Martinsson
Data analysis and interpretation: Gudrun Schleiermacher, Niloufar Javanmardi, Virginie Bernard, Quentin Leroy, Julie Cappo, Thomas Rio Frio, Olivier Delattre, Tommy Martinsson
Manuscript writing: All authors
Final approval of manuscript: All authors

REFERENCES

1. Hanahan D, Weinberg RA: Hallmarks of cancer: The next generation. Cell 144:646-674, 2011
2. Ding L, Ley TJ, Larson DE, et al: Clonal evolution in relapsed acute myeloid leukaemia revealed by whole-genome sequencing. Nature 481:506-510, 2012
3. Landau DA, Carter SL, Stojanov P, et al: Evolution and impact of subclonal mutations in chronic lymphocytic leukemia. Cell 152:714-726, 2013
4. Schuh A, Becq J, Humphray S, et al: Monitoring chronic lymphocytic leukemia progression by whole genome sequencing reveals heterogeneous clonal evolution patterns. Blood 120:4191-4196, 2012
5. Welch JS, Ley TJ, Link DC, et al: The origin and evolution of mutations in acute myeloid leukemia. Cell 150:264-278, 2012
6. Maris JM, Hogarty MD, Bagatell R, et al: Neuroblastoma. Lancet 369:2106-2120, 2007
7. Janoueix-Lerosey I, Schleiermacher G, Michels E, et al: Overall genomic pattern is a predictor of outcome in neuroblastoma. J Clin Oncol 27:1026-1033, 2009
8. Molenaar JJ, Koster J, Zwijnenburg DA, et al: Sequencing of neuroblastoma identifies chromothripsis and defects in neuritogenesis genes. Nature 483:589-593, 2012
9. Pugh TJ, Morozova O, Attiyeh EF, et al: The genetic landscape of high-risk neuroblastoma. Nat Genet 45:279-284, 2013
10. Sausen M, Leary RJ, Jones S, et al: Integrated genomic analyses identify ARID1A and ARID1B alterations in the childhood cancer neuroblastoma. Nat Genet 45:12-17, 2013
11. Schleiermacher G, Janoueix-Lerosey I, Ribeiro A, et al: Accumulation of segmental alterations determines progression in neuroblastoma. J Clin Oncol 28:3122-3130, 2010
12. Carén H, Abel F, Kogner P, et al: High incidence of DNA mutations and gene amplifications of the ALK gene in advanced sporadic neuroblastoma tumours. Biochem J 416:153-159, 2008
13. De Brouwer S, De Preter K, Kumps C, et al: Meta-analysis of neuroblastomas reveals a skewed ALK mutation spectrum in tumors with MYCN amplification. Clin Cancer Res 16:4353-4362, 2010
14. Hallberg B, Palmer RH: Mechanistic insight into ALK receptor tyrosine kinase in human cancer biology. Nat Rev Cancer 13:685-700, 2013
15. Janoueix-Lerosey I, Lequin D, Brugieres L, et al: Somatic and germline activating mutations of the ALK kinase receptor in neuroblastoma. Nature 455:967-970, 2008
16. Mossé YP, Laudenslager M, Longo L, et al: Identification of ALK as a major familial neuroblastoma predisposition gene. Nature 455:930-935, 2008
17. Schulte JH, Lindner S, Bohrer A, et al: MYCN and ALKF1174L are sufficient to drive neuroblastoma development from neural crest progenitor cells. Oncogene 32:1059-1065, 2013
18. Barone G, Anderson J, Pearson AD, et al: New strategies in neuroblastoma: Therapeutic targeting of MYCN and ALK. Clin Cancer Res 19:5814-5821, 2013
19. Bresler SC, Wood AC, Haglund EA, et al: Differential inhibitor sensitivity of anaplastic lymphoma kinase variants found in neuroblastoma. Sci Transl Med 3:108ra114, 2011
20. Carpenter EL, Mossé YP: Targeting ALK in neuroblastoma: Preclinical and clinical advancements. Nat Rev Clin Oncol 9:391-399, 2012
21. Mossé YP, Lim MS, Voss SD, et al: Safety and activity of crizotinib for paediatric patients with refractory solid tumours or anaplastic large-cell lymphoma: A Children's Oncology Group phase 1 consortium study. Lancet Oncol 14:472-480, 2013
22. Martinsson T, Eriksson T, Abrahamsson J, et al: Appearance of the novel activating F1174S ALK mutation in neuroblastoma correlates with aggressive tumor progression and unresponsiveness to therapy. Cancer Res 71:98-105, 2011
23. Ihle MA, Fassunke J, Konig K, et al: Comparison of high resolution melting analysis, pyrosequencing, next generation sequencing and immunohistochemistry to conventional Sanger sequencing for the detection of p.V600E and non-p.V600E BRAF mutations. BMC Cancer 14:13, 2014
24. Monzon FA, Ogino S, Hammond ME, et al: The role of KRAS mutation testing in the management of patients with metastatic colorectal cancer. Arch Pathol Lab Med 133:1600-1606, 2009
25. Liu L, Li Y, Li S, et al: Comparison of next-generation sequencing systems. J Biomed Biotechnol 2012:251364, 2012
26. Ross MG, Russ C, Costello M, et al: Characterizing and measuring bias in sequence data. Genome Biol 14:R51, 2013

Affiliations

Gudrun Schleiermacher, Julie Cappo, Isabelle Janoueix-Lerosey, and Olivier Delattre, L'Institut National de la Santé et de la Recherche Médicale U830, Laboratoire de Génétique et Biologie des Cancers; Gudrun Schleiermacher, Virginie Bernard, Quentin Leroy, Thomas Rio Frio, Gaelle Pierron, Eve Lapouble, and Jean Michon, Institut Curie; Michel Peuchmaur, Assistance Publique–Hôpitaux de Paris, Hôpital Universitaire Robert Debré, Service de Pathologie; Michel Peuchmaur, Université Diderot Paris 7, Sorbonne Paris-Cité, Paris; Valérie Combaret, Centre Léon-Bérard, Laboratoire de Recherche Translationnelle, Lyon, France; Niloufar Javanmardi, Anna Djos, Jonas Abrahamsson, and Tommy Martinsson, The Sahlgrenska Academy, University of Gothenburg, Sahlgrenska University Hospital, Gothenburg; Ingrid Øra, Lund University, Lund; Fredrik Hedborg, Uppsala University, and Centre for Research and Development, Uppsala University/County Council of Gävleborg, Gävle; Catarina Träger and Per Kogner, Karolinska Institute, Astrid Lindgren Children's Hospital, Stockholm; Britt-Marie Holmqvist, Linköping University Hospital, Linköping, Sweden; Frank Speleman and Bram de Wilde, Center for Medical Genetics, Ghent University Hospital, Ghent, Belgium.

Acknowledgment

We thank the following colleagues for their contribution to this study: Isabelle Aerts, Nathalie Clement, Carole Coze, Anne-Sophie Defachelles, Sandrine Ferrand, Paul Frénaux, Geneviève Laureys, Philippe Lemoine, Aurélien Marabelle, Pascale Philippe-Chomette, Dominique Plantaz, Hervé Rubie, Estelle Thebaud, Jo Vandesompele, and Nadine Van Roy. We also thank the Centre des Ressources Biologiques of Centre Leon Berard, Lyon, France.